Materials Physics and Mechanics 42 (2019) 407-414 Received: November 28, 2018

ROTARY ACTUATOR CONTROL BASED ON TENSILE FORCE ELEMENTS MADE OF SHAPE MEMORY Cu–Al–Ni CRYSTALS WHEN OPERATED IN A CYCLIC MODE

A.I. Priadko[1*], S.A. Pulnev[1], O.O. Kovalev[2,3], I.A. Ilin[2]

[1]Ioffe Institute, Polytechnicheskaya 26, St. Petersburg, 194021, Russian Federation

[2]Peter the Great St.Petersburg Polytechnic University, Polytechnicheskaya str. 29,

St. Petersburg, 195251, Russian Federation

[3]Turner Scientific Research Institute for Children's Orthopedics,

Parkovaya str. 64-68, Pushkin, St. Petersburg, 196603, Russia

*e-mail: aiprdko@mail.ru

Abstract. An actuator design and a function scheme are developed. A control algorithm of a cyclic actuator is considered. We provide experimental results on the control algorithm and the actuator. The actuator operating range is 60°. The actuator sped is ~ 1 degree/second. The actuator operating is stable in any rotation angle in operating range.

Keywords: shape memory effect, Cu–Al–Ni single crystals, cyclic rotary actuator

1. Introduction

Shape memory materials undergoing martensitic transformations induced by an external force can be subjected to large deformations of inelastic nature, and, as a result, to a change of the initial shape of a specimen. Such deformations may have different types, e.g., tension, compression, torsion or bend. The recovery effect of accumulated inelastic strain resulting into attaining the original shape of the specimen, both, can occur during unloading processes at a constant temperature (superelasticity effect), or upon heating (shape memory effect). These reversible deformations can scale from several percent to several tens percent [1-2].

When we consider a shape memory effect caused by heating, we observe reverse martensitic transformation. In the presence of external loads resisting the shape recovery it generates stress in a specimen and, as a result, induces reactive force field, which counteracts the external force [3-5]. If the counter force significantly surpasses the force caused by an initial strain, one can possibly make use of the gained mechanical work in various technical devises based on the shape memory effect [6]. It is expected that the cyclic actuator has zero or very small magnitude of irreversible plastic deformations in shape memory elements working under periodical thermal and mechanical loads.

In our previous works [7-8] we considered properties of Cu-Al-Ni single crystals to design cyclic linear motors based on the shape memory effect. In this paper we aim to develop a cyclic rotary actuator, its design and a control system. The work also presents the results of testing the assembled engine operating in cyclic mode.

2. Design of the actuator

Adopting the principles outlined in previous works [7-11], the cyclic rotary actuator based on elastic force elements was designed and manufactured. A 3D model of the actuator is shown

http://dx.doi.org/10.18720/MPM.4242019_5

in Fig. 1a and a manufactured actuator in Fig. 1b. The actuator consists of two force elements based on Cu–Al–Ni with individual electric heating elements (not shown on Fig. 1); the shaft is mounted in two rolling bearings and supporting body. An angle sensor of shaft rotation is attached on the body of the actuator with a clutch. Each force element swivel is connected to the actuator body by a sleeve and the shaft on one end. Another end is connected by sleeve to a lever, which rigidly fixed by an output shaft.

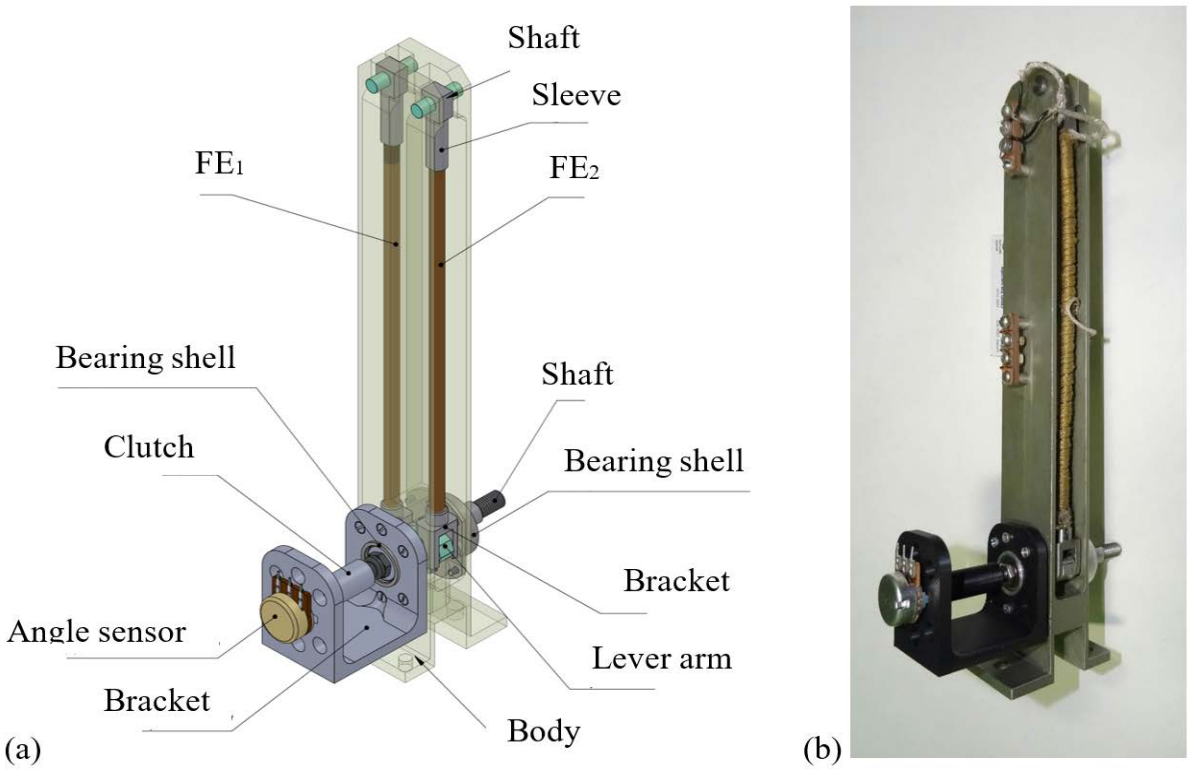

Fig. 1. Actuator a) 3D model, b) prototype

Force element (further FE) made of cylindrical rod with 3 mm diameter and 160 mm length has 6 mm screw-thread on each end to connect with an actuator body. Each FE has its own spiral electric heating element. The heating element consists of a nichrome wire in silica wicker isolation. The thermocouple installed on the rod center between the spirals of the heating element, and coated by the thermal conductive paste.

Main parameters of the actuator are shown in Table 1.

Table 1. Actuator parameters

	Designation	Value	Units
Diameter of FE	d	3	mm
Length of undeformed FE	L	148	mm
Reversible deformations	ε_{SM}	0.08	
Heating element power	P	135	W
Operating temperature	T	60 - 200	ºC
Type of thermocouple		Chromel–Copel	

3. Actuator control in the cyclic mode

For realization of the cyclic work of the actuator it is necessary to organize the «heating – cooling» cycle for each FE. FE should be connected as follows; when one element contracts,

it seeks to compensate the external load and deforms the second element. As a result, the second element is ready to contract on the next step of the work cycle.

Figure 2 shows the rotary actuator scheme. The actuator consists of two force elements FE_1 and FE_2. Each FE is connected to the actuator body by a joint and a shaft at one end. Another end is connected by a joint to a lever, which is rigidly fixed by an output shaft. The output shaft is installed on bearing supports.

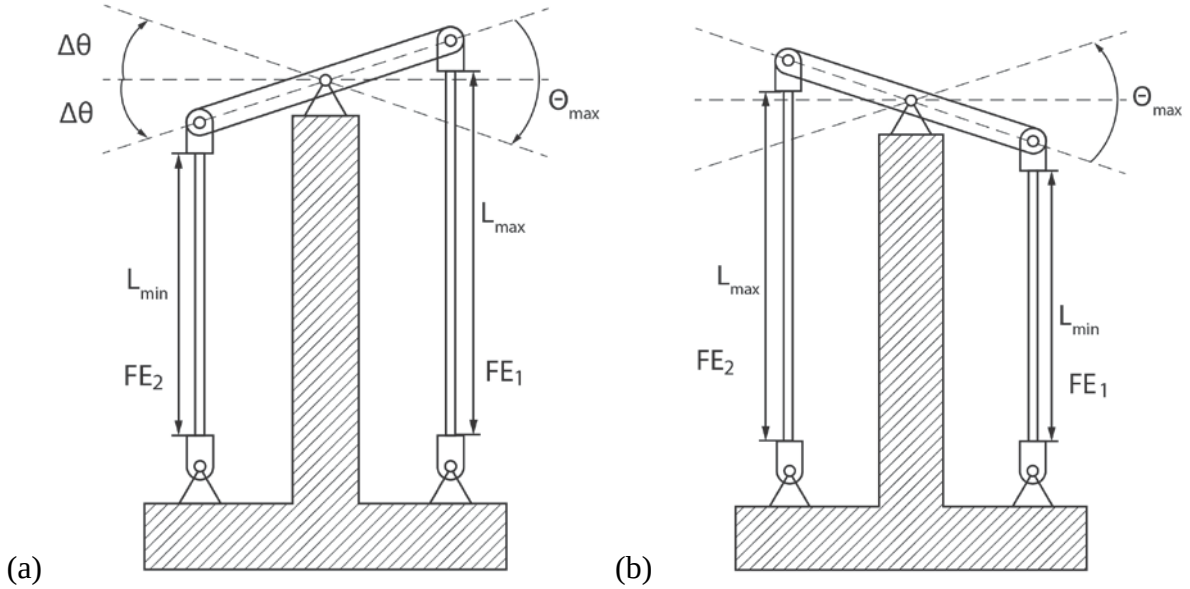

Fig. 2. A scheme of the cyclic rotary actuator; an initial position of the actuator without load (a), the final position of the actuator (b)

Figure 2a shows an initial position of the actuator shaft. In this position FE_1 reaches its maximum deformation level ($\varepsilon_1 = \varepsilon_{sm}$) and its length L_{max}, whereas FE_2 has zero deformation ($\varepsilon_2 = 0$) and minimal length L_{min}. The lever makes angle $-\Delta\theta$ with the horizon (its medium position). In the medium position the deformation and length of FE_1 and FE_2 are the same:

$$\varepsilon_1 = \varepsilon_2 = \frac{1}{2}\varepsilon_{sm}, \tag{1}$$

$$L_1 = L_2 = \frac{1}{2}(L_{min} + L_{max}) = L_{min}\left(1 + \frac{1}{2}\varepsilon_{sm}\right). \tag{2}$$

Figure 2b shows the final position of the actuator. Due to the heating of FE_1, it returns to the initial length L_{min} and acquires zero deformation state ($\varepsilon_1 = 0$). In heating process of FE_1 the shaft, as it's shown Fig. 2a, turns at angle $\Theta_{max} = 2\Delta\theta$ clockwise and elongates FE_2 to length L_{max} with deformations $\varepsilon_2 = \varepsilon_{sm}$. For performing of a full cycle, it is necessary to return shaft to its initial position by a counter-clockwise rotation at angle Θ_{max} by heating FE_2 and cooling FE_1 simultaneously.

Figure 3 shows the relations between deformations $[\varepsilon_1, \varepsilon_2]$ and lengths $[L_1, L_2]$ of FE and the shaft rotation angle θ (Fig. 2a).

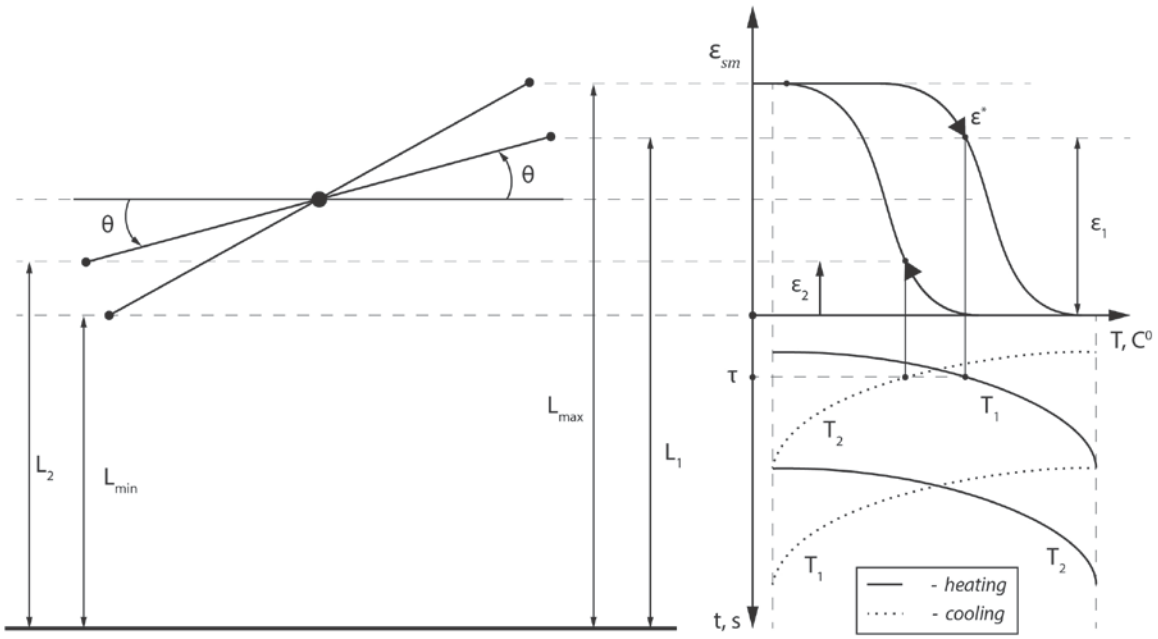

Fig. 3. Functional parameters of the engine cyclic operation

Diagram in Fig. 3 shows the initial position of the actuator along with its position at moment τ. For the initial position, the values are:

$$\varepsilon_1^0 = \varepsilon_{max},\ \ \varepsilon_2^0 = 0, \tag{3}$$

$$L_1^0 = L_1 = L_0(1 + \varepsilon_{max}), L_2^0 = L_0. \tag{4}$$

Heating FE_1 results into the loss of its deformation ε^* at moment τ.

Due to FEs change their lengths consistently, so the deformations of elements are:

$$\varepsilon_1 + \varepsilon_2 = \varepsilon_{sm}. \tag{5}$$

Thus we arrive at the following relation

$$\varepsilon_1(\tau) = \varepsilon_{max} - \varepsilon^*(\tau), \varepsilon_2(\tau) = \varepsilon_{max} - \varepsilon_1(\tau) = \varepsilon^*(\tau), \tag{6}$$

$$L_1(\tau) = L_0\big(1 + \varepsilon_{max} - \varepsilon^*(\tau)\big), L_2(\tau) = L_0\big(1 + \varepsilon^*(\tau)\big), \tag{7}$$

$$|\theta(\tau)| = \frac{\left|L_0\left(1+\frac{1}{2}\varepsilon_{max}\right) - L_i(\tau)\right|}{R},\ i = 1, 2, \tag{8}$$

where R is the length of the lever.

4. Actuator control system

Actuator control system consists of the following elements: PC, Arduino Uno, control software, power supply for 270W, DC–DC stabilizer for 5V, two k-type thermocouples, two amplifiers for thermocouples, and two high current transistors.

The control system is organized in following manner; the power supply 270W is used to heat FE_1 and FE_2; DC–DC 5V stabilizer is used to power up the control system; the heating temperature of rods is set as parameters in the control software; the temperature of rods is measured by the thermocouples, installed at the center of the shape memory elements. Signals from the thermocouples are sent to the amplifier and then to Arduino. Controller sends PWM signals to the transistors and regulates power supply for the heaters regarding to the temperature of FEs. Rotation angle is measured by a potentiometer connected to the output shaft.

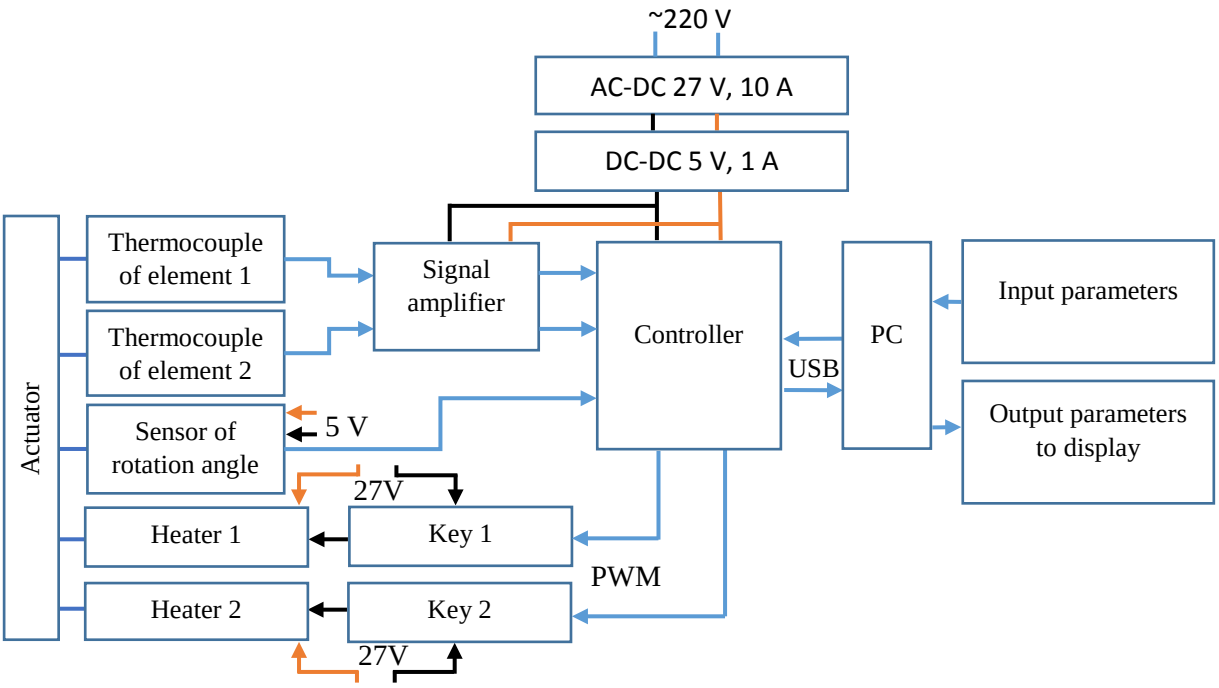

Fig. 4. Function scheme of control system of actuator

5. A control algorithm for the cyclic mode driver

Setting temperature and angle. The actuator cycles are controlled by MatLab script. Standard package "MatLab Support Package for Arduino Hardware" was used to communicate through Serial-USB port with microcontroller Arduino Uno.

The desired temperature is assigned to the each element, namely FE_1 and FE_2 by a MatLab script. The evaluated power in the range of 0-135W is supplied to each of the heaters using a PI controller (proportional-integral controller) to achieve the desired temperature. The scheme of temperature regulator working is shown in Fig. 5.

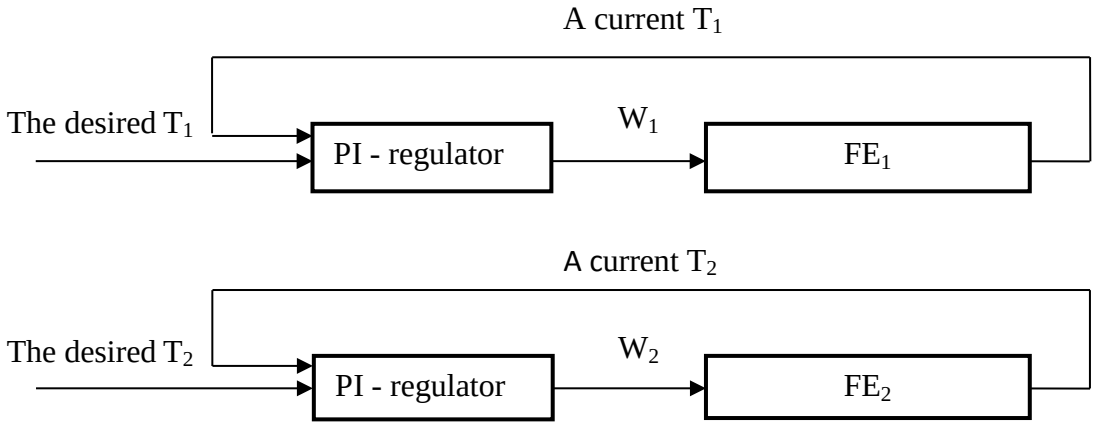

Fig. 5. Temperature control scheme

For actuators working in the cyclic mode, the FE_1 and FE_2 were heated and cooled one by one.

The cyclic mode without a load. The hearting of FE_1, FE_2 is realizing by PI – regulator, which was described before. On the first experiment (Fig. 6) for hysteresis loop selected 70°C – 170°C bound conditions. FE1 and FE2 are located on different tips of hysteresis loop (FE1 have 70°C, FE2 have 170°C) at initial time. The actuator rotation is starting, when we start a cooling FE with 170°C temperature and heating the other FE with 70°C temperature. The cooling and the heating have the same heat flow speed. The cooling occur by contact with 24°C air. As bigger speed of the cooling of one FE, as bigger the heating speed of another FE and as bigger a rotation speed.

A diapason of the actuator shaft rotation is from 0° to 60°. The shaft rotation has maximum speed below 3° and 53°. In this diapason, the angle changes linearly.

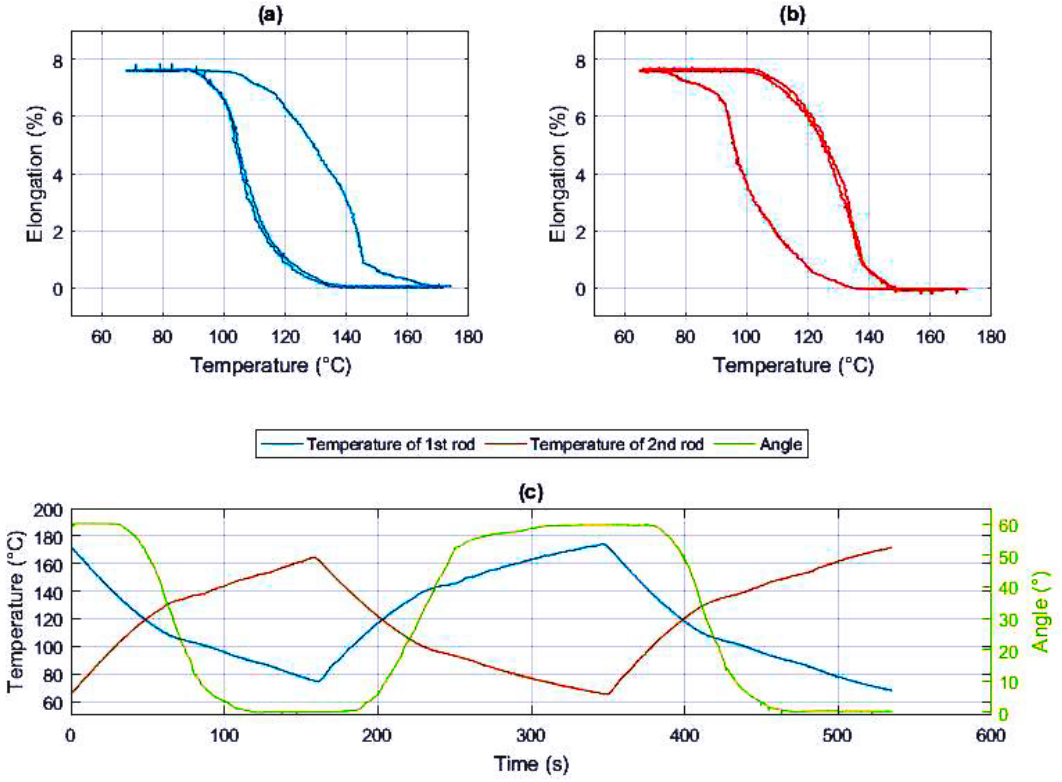

Fig. 6. The cyclic mode in 70°C – 170°C range: (a) FE_1 hysteresis loop, (b) FE_2 hysteresis loop, (c) A changes of FE_1, FE_2 temperatures and the angle of shaft rotation by time

On the second experiment (Fig. 7) for hysteresis loop selected 95°C – 145°C bound conditions. In this case, hysteresis loop lose some areas of their tips (as shows Fig. 7a,b). This kind of hysteresis loop bound conditions make possible to reaches the maximum speed of the shaft rotation of the actuator.

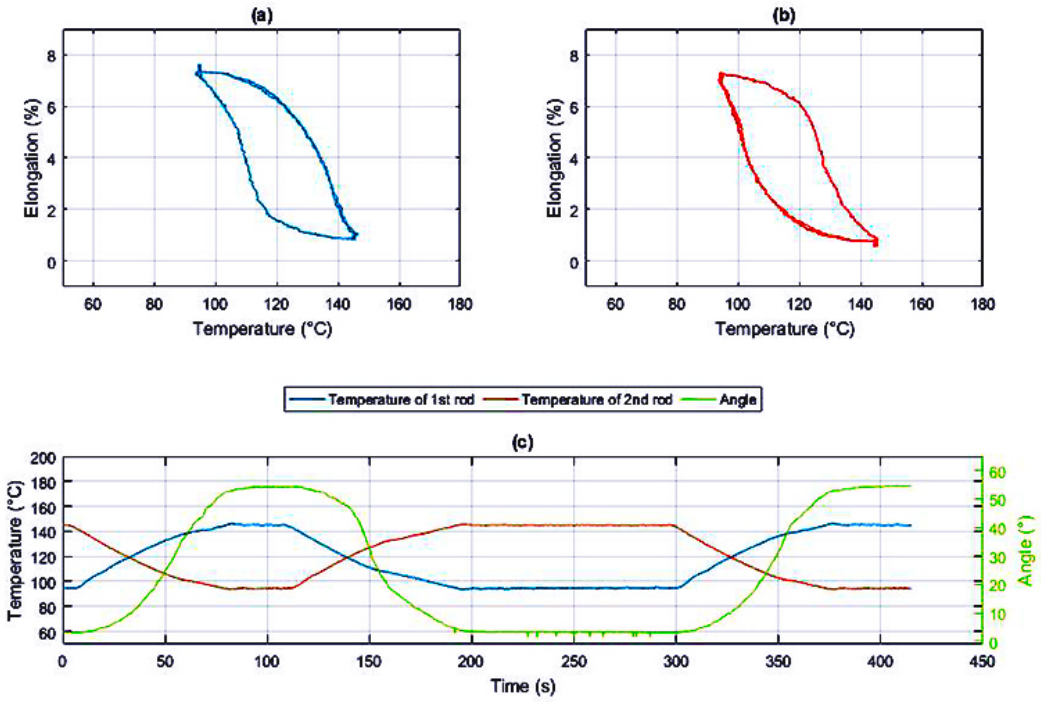

Fig. 7. The cyclic mode in 95°C – 145°C range: (a) FE_1 hysteresis loop, (b) FE_2 hysteresis loop, (c) A changes of FE_1, FE_2 temperatures and the angle of shaft rotation by time

On the third experiment (Fig. 7) for hysteresis loop selected 95°C – 135°C bound conditions. In this case, hysteresis loop has less deformation (as shows Fig. 7a,b). The only 10°C changes in bound conditions provide 2% lose in deformation and as result, we have 20°-43° rage of the angle of the shaft rotation.

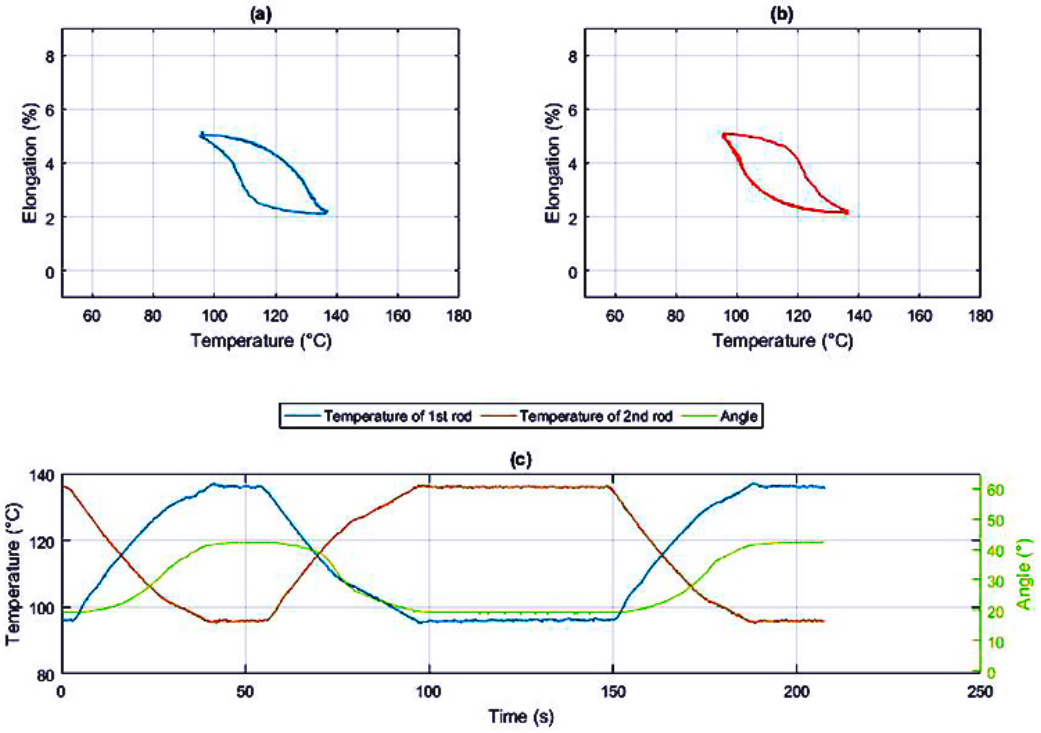

Fig. 8. The actuator testing in 95°C – 135°C: a) dependents of FE_1 and temperature b) dependents of FE_2 and temperature, c) dependents of FE_1, FE_2 elements and angle rotation

Conclusion

The cyclic rotary actuator was designed and made. The control algorithm of the cyclic actuator was considered. We provided experimental results on the control algorithm and the actuator. The diagrams of the cyclic mode without a load show dependents of the actuator parameters and the hysteresis loop bound conditions. We can realize the desired actuator mode by changing of this bound conditions and the cooling speed. If the conditions are the same, the each cycle of the actuator is the same and does not change by time. The next steps are investigation of the cyclic mode by load and a positioning of the shaft rotary angle. The results of this work have been applied in bionic prosthesis design in project by SPbPU.

Acknowledgements. *This work was supported by the Russian Science Foundation under Project 16–19– 00129.*

References

[1] Horikawa H, Ichinose S, Moorii K, Miyazaki S, Otsuka K. Orientation dependence of β→β` stress-induced martensitic transformation in a Cu-Al-Ni alloy. *Metallurgical Transactions A.* 1988;19(4): 915-923.

[2] Jani JM, Leary M, Subic A, Gibsone MA. A review of shape memory alloy research, applications and opportunities. *Materials and Design.* 2014;56: 1078-1113.

[3] Pulnev SA, Nikolaev VI, Malygin GA, Kuzmin SL, Shpeizman VV, Nikanorov SP. Generation and relaxation of reactive stresses in Cu-Al-Ni shape-memory alloy. *Technical Physics.* 2006;51(8): 1004-1007.

[4] Nikolaev VI, Pulnev SA, Malygin GA, Shpeizman VV, Nikanorov SP. Generation and relaxation of reactive stresses in a Cu-Al-Ni shape memory alloy upon cyclic temperature variation in the range 293-800 K. *Physics of the Solid State.* 2008;50(11): 2170-2174.

[5] Nikolaev VI, Averkin AI, Egorov VM, Malygin GA, Pulnev SA. Influence of incomplete shape memory deformation on the generation of reactive stresses in single crystals of the Cu-Al-Ni alloy. *Physics of the Solid State.* 2014;56(3): 522-526.

[6] Pulnev S, Nikolaev V, Priadko A, Rogov A, Viahhi I. Actuators and Drivers Based on CuAlNi Shape Memory Single Crystals. *Journal of Materials Engineering and Performance*. 2010;20(4-5): 497-499.

[7] Priadko AI, Pulnev SA, Nikolaev VI, Rogov AV, Shmakov OA, Golyandin SN, Chikiryaka AV. Investigation of single crystal Cu-Al-Ni alloy bending force elements for linear motors. *Materials Physics and Mechanics.* 2016;29(2): 158-165.

[8] Priadko AI, Nikolaev VI, Pulnev SA, Stepanov SI, Rogov AV, Chikiryaka AV, Shmakov OA. Shape memory Cu-Al-Ni single crystals for application in rotary actuators. *Materials Physics and Mechanics.* 2017;32(1): 83-87.

[9] Belyaev SP, Voitenko YV Kuzmin SL, Likhachev VA, Kovalev VM. Cyclic shape memory and the operating capacity of titanium nickelide. *Strength of Materials.* 1989;21(6): 748-752.

[10] Belousov VL, Dukin AD, Favstov YK. Executive mechanism of multiple action with reciprocating motion. In: *Materials with the effect of shape memory and their application.* Novgorod: 1989. p.191-192.

[11] Ostapenko AV. Efficiency of martensitic engines and methods for increasing it. In: *Materials with the shape memory effect and their application.* Novgorod: 1979. p.125-129.